



Co-published by
Institute of Fluid-Flow Machinery
Polish Academy of Sciences
and
Committee on Thermodynamics and Combustion
Polish Academy of Sciences

<http://www.imp.gda.pl/archives-of-thermodynamics/>



Flow maps in multiphase flows

Małgorzata Sikora^{a*}, Tadeusz Bohdal^a, Stanisław Witczak^b, Grzegorz Ligus^b

^aPolitechnika Koszalińska, Katedra Energetyki, ul. Śniadeckich 2, 75-453 Koszalin, Poland

^bKatedra Inżynierii Procesowej i Środowiska, Politechnika Opolska, ul. St. Mikołajczyka 5, 45-271 Opole, Poland

*Corresponding author email: malgorzata.sikora@tu.koszalin.pl

Received: 23.01.2024; revised: 18.03.2024; accepted: 09.04.2024

Abstract

Flow structure maps are the most useful tool in the process of identifying structures formed in multiphase flows. They can be defined as a graphical way to present the transition boundaries of flow structures, depending on the characteristic parameters of the phase transformation or flow, such as the vapor quality, the void fraction, the mass flow density, or the velocities of individual phases. Maps are usually two-dimensional drawings, described with a minimum of two selected parameters or quantities describing the phenomenon. The oldest maps of flow structures concerned adiabatic flows, mainly two-phase water-air systems or three-phase water-oil-air systems in conventional channels. Maps of nonadiabatic flow structures are simple and allow the selection of an appropriate model to determine the heat transfer coefficient as well as the flow resistance of the refrigerant. This has a major impact on the design of flow devices, where two- and even three-phase flows. This paper includes reviews of proposed maps of multiphase flow structures by various authors.

Keywords: Multiphase flows; Flow structures; Flow maps

Vol. 45(2024), No. 2, 19–28; doi: 10.24425/ather.2024.150848

Cite this manuscript as: Sikora, M., Bohdal, T., Witczak, S., & Ligus, G. (2024). Flow Maps in Multiphase Flows. *Archives of Thermodynamics*, 45(2), 19–28.

1. Introduction

The term "two-phase flow" of a refrigerant means the flow of two phases in a system of any geometry. A distinction can be made between a continuous phase (liquid or gas) and a dispersed phase (liquid, gas or solid). The dispersed phase occurs in the form of drops, bubbles or particles and is suspended in the continuous phase. A phase boundary separates both phases. During two-phase flow, the phase separation boundary changes its shape and thus various two-phase flow structures are created. The situation is similar in the case of three-phase flow structures, but in this case, there are more possibilities for phase configura-

tion. In this case, the phases in the flow are two immiscible liquids and a gas, or less commonly a liquid, a gas and a solid.

Figures 1 and 2 show examples of two-phase flow structures occurring in horizontal and vertical channels [1–3]. Some of these structures disappear when the channel diameter decreases or the mass flow density G increases. In the case of flows in vertical channels, the flow structures depend on the flow direction and the mutual density ratio of both phases. The relationship between the formation of water-oil flow structures depending on the flow velocity is shown in Fig. 3 [4]. As can be seen, at higher velocities the structures combine into larger agglomerates.

Nomenclature

- A – cross section area, m^2
- d – internal diameter, mm
- G – mass flux density, $kg/(m^2s)$
- j – apparent velocity, m/s
- L – length, m
- q – heat flux, W/m^2
- T – temperature, $^{\circ}C$
- u – apparent velocity, m/s
- \dot{V} – volume flow, m^3/s
- x – vapour quality

Greek symbols

- λ – coefficient defined by Baker, $\lambda_B = \frac{\rho_v \cdot \rho_l}{\sqrt{\rho_p \cdot \rho_w}}$
- μ – viscosity, $Pa \cdot s$

- ρ – density, kg/m^3
- σ – surface tension, N/m
- ϕ – void fraction
- χ_{IT} – Lockhart Martinelly parameter

ψ – coefficient defined by Baker, $\psi_B = \frac{\sigma_w}{\sigma_l} \left[\frac{\mu_l}{\mu_w} \left(\frac{\rho_w}{\rho_l} \right)^2 \right]^{1/3}$

Subscripts and Superscripts

- g,o – gas-oil domination
- h – hydraulic
- l – liquid
- o,o – oil domination
- s – saturation
- v – vapour
- w – water
- w,o – water-oil domination
- $3F,o$ – three-phase flow with dominant oil

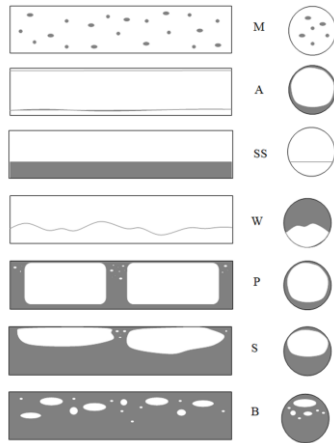


Fig. 1. Schematic diagram of two-phase adiabatic flow in conventional horizontal channel: M – mist flow, A – annular, SS – stratified, W – wavy, S – slug, P – plug, B – bubbly [1].

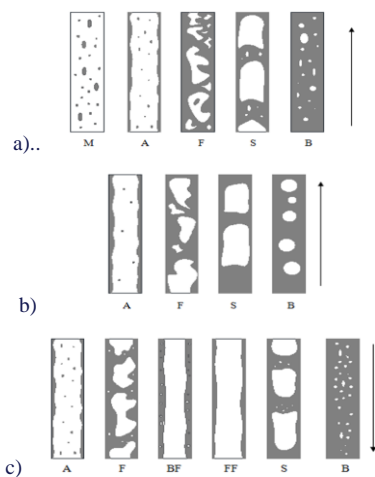


Fig. 2. Schematic diagram of two-phase adiabatic flow in the conventional vertical channel by Dziubiński and Prywer [2] and Ulbrich [3]: a) upflow; b) upflow involving a very viscous fluid; c) downflow. M – mist flow, A – annular, F – frothy, S – slug, B – bubbly, FF – liquid film flow, BF – bubbly-film.

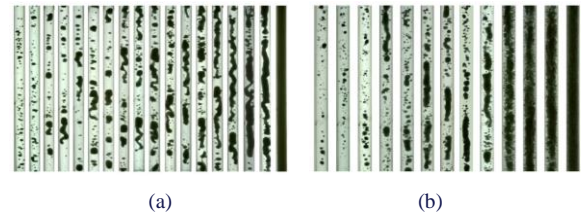


Fig. 3. Structures of water-oil upflow by Zhang et al. [4]: (a) $v = 0.28$ m/s; (b) $v = 0.57$ m/s.

Figure 4 shows the three-phase upflow structures for vertical channels published by Bannwart et al. [5]. They isolated an annular flow A with an oil core and gas bubbles in water forming the ring. They also observed the occurrence of an intermittent structure I, where gas bubbles are separated by oil, and water in the form of a thin layer that adheres to the channel wall.

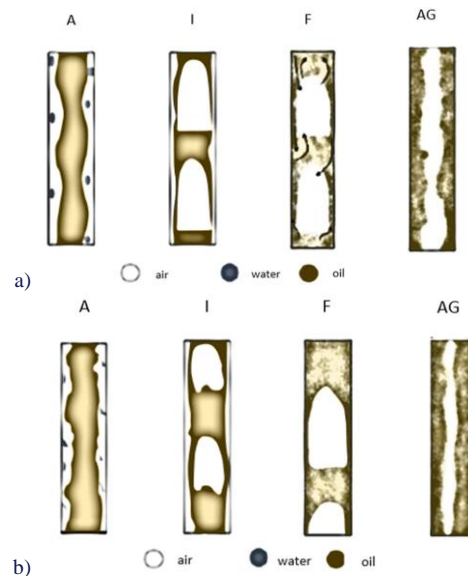


Fig. 4. Three-phase upflow structures air-water-petroleum flow in the vertical channel by Bannwart et al. [5]: a) $d = 28.4$ mm; b) $d = 10$ mm.

Another type of flow is the frothy structure F, in which the flow is pulsating and it is difficult to distinguish the liquid phases that mix. The occurrence of an annular gas phase AG was also observed, where a mixture of small oil and water droplets flows on the wall, and gas flows through the middle of the channel. At high velocities, the water and oil mixture may form an emulsion [6]. The same authors published the structures of three-phase water-oil-air flow in horizontal channels, shown in Fig. 5.

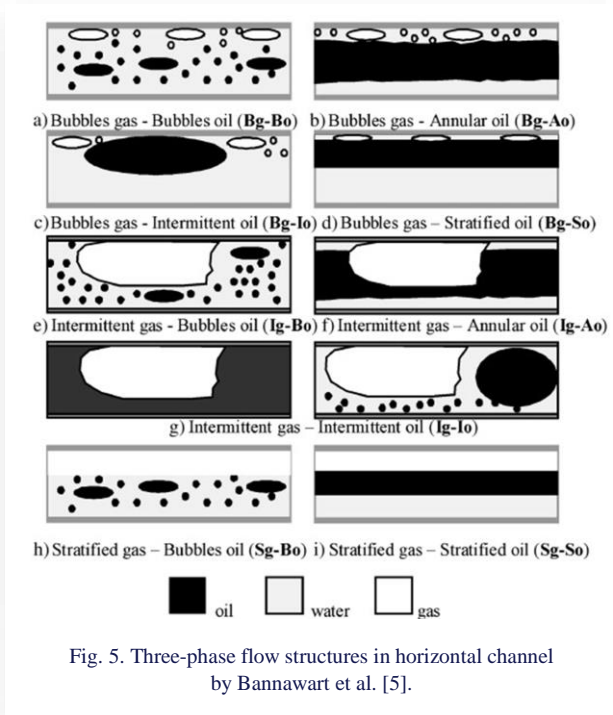


Fig. 5. Three-phase flow structures in horizontal channel by Bannawart et al. [5].

2. Maps of two-phase flow structures

Flow structure maps are the most useful tool in the process of identifying structures formed in multiphase flows. A flow structure map is a graphical way of presenting the transition boundaries of flow structures, depending on the flow parameters. They are two-dimensional drawings, described with a minimum of two characteristic parameters or quantities describing the phenomenon. The oldest maps of flow structures concerned adiabatic flows, mainly the water-air system in conventional channels.

Two-phase flow is the flow of two immiscible substances or the same substance in different states of matter in one system. Two-phase flows can be divided into adiabatic (without heat exchange) and non-adiabatic (phase changes of condensation and boiling).

2.1. Adiabatic flow

The most common adiabatic flows in the literature are liquid-liquid (e.g. water-oil) or liquid-gas flows (water-air). Liquid-liquid flows are most often implemented in horizontal and vertical channels with upflow or downflow. The first published flow map was Baker's map (Fig. 6) [7]. The oldest map of the rising

flow of liquid-liquid mixtures in a vertical channel was published by Charles et al. [8], it is a map of the two-phase oil-water mixture, presented in Fig. 7a. Figure 7b shows a map of the flow in a vertical pipe of a mixture of water and oil with a density higher than the density of water, published by Troniewski et al. [9] and Xu et al. [10] modified the two-phase liquid-liquid flow maps by Flores [11] in vertical ascending and descending flow. Figure 8 shows Flores' maps with the red modification by Xu et al. [10]. These maps were prepared for the oil-water flow at the density ratio $\rho_o/\rho_w = 0.85$ and the channel diameter $d = 50.8$ mm, where the transitional flow was marked as C.

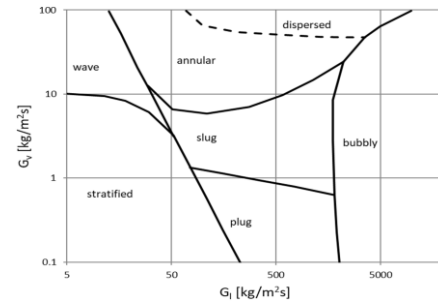


Fig. 6. Two-phase flow map by Baker [7].

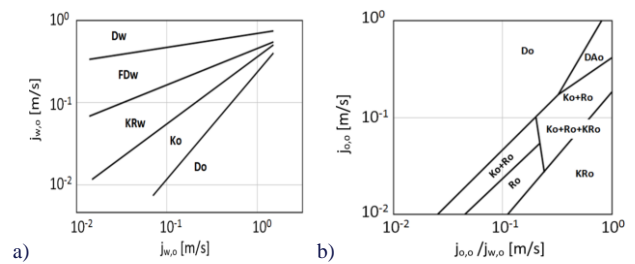


Fig. 7. Maps of liquid-liquid flow by: a) Charles et al. [8]; b) Troniewski et al. [9]. Dw – dispersive flow of water, Do – dispersive flow of oil, DAo – dispersive – annular flow of oil, FDw – film-dispersion water flow, KRw – droplet-slug flow of water, Ko – droplet oil flow, KRo – droplet-slug flow of oil, Ro – stratified oil flow [12].

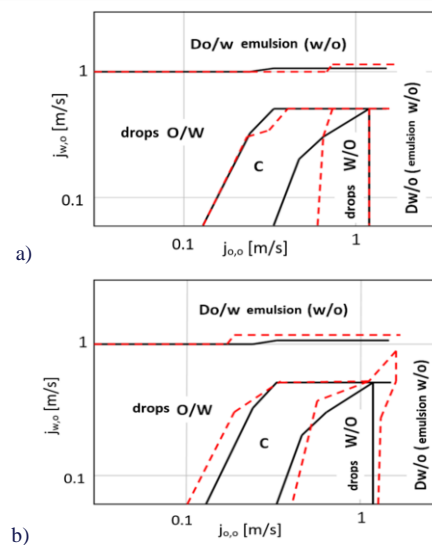


Fig. 8. Maps of vertical two-phase flow by Flores [11] and Xu et al. [10]:

A more frequently studied case of two-phase adiabatic flow is the water-air flow. Hawitt and Roberts [13] proposed a map of the adiabatic upflow during the two-phase flow of a mixture of water and air in vertical channels with a hydraulic diameter of $d = 10$ and 30 mm, shown in Fig. 9a. To describe the boundaries of the flow structures, the densities ρ and apparent velocities j of individual phases were used:

$$j_l = \frac{\dot{V}_l}{A}, \quad (1)$$

$$j_v = \frac{\dot{V}_v}{A}. \quad (2)$$

The most popular map in comparative analysis of two-phase flow structures is the map of Taitel and Dukler [14] presented in Fig. 9b.

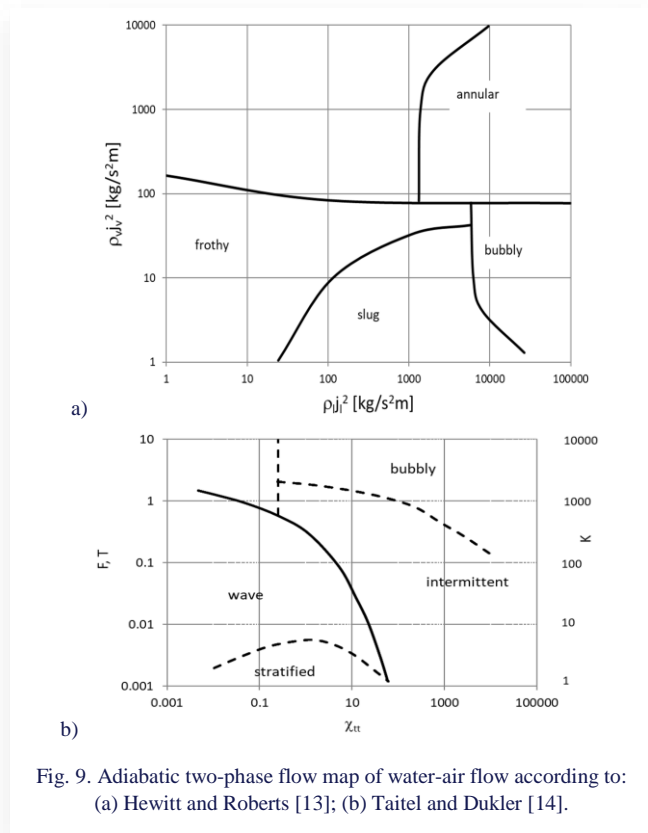


Fig. 9. Adiabatic two-phase flow map of water-air flow according to: (a) Hewitt and Roberts [13]; (b) Taitel and Dukler [14].

The map was developed for two-phase adiabatic systems in the range of hydraulic diameter $d = 4.8$ – 22 mm, mass flow density $G = 18$ – 990 $\text{kg}/(\text{m}^2 \cdot \text{s})$ and pressure $p = 108$ – 1249 kPa [12]. Four characteristic quantities marked with the symbols: F , T , K and Y were used in the construction of this map. These are functions of the Lockhart - Martinelli parameter χ_{tt} , determined as follows:

$$F = \frac{j_v}{(d_h g \cos\theta)^{0.5}} \cdot \left(\frac{\rho_v}{\rho_l - \rho_v} \right)^{0.5}, \quad (3)$$

$$T = \left[\frac{(dp/dz)_l}{(\rho_l - \rho_v) g \cos\theta} \right]^{0.5}, \quad (4)$$

$$\chi_{tt} = \left(\frac{1-x}{x} \right)^{0.875} \cdot \left(\frac{\rho_v}{\rho_l} \right)^{0.5} \cdot \left(\frac{\mu_l}{\mu_v} \right)^{0.125}. \quad (5)$$

Figure 10a shows a map of the structures of a two-phase, adiabatic flow in a horizontal channel, and Fig. 10b shows a map of the upflow structures in a vertical channel by Ulbrich [15].

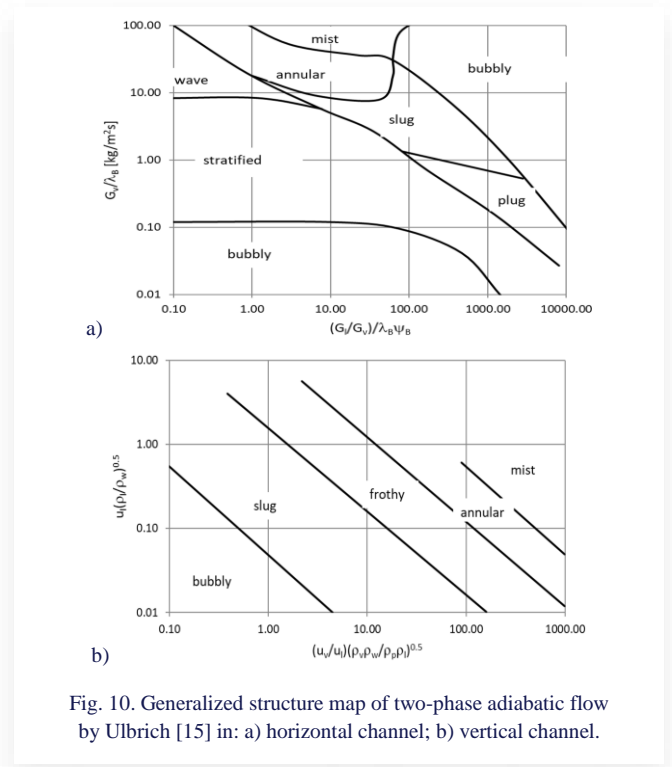


Fig. 10. Generalized structure map of two-phase adiabatic flow by Ulbrich [15] in: a) horizontal channel; b) vertical channel.

2.2. Nonadiabatic flow

Flow structures during condensation or boiling differ significantly from those observed in two-phase adiabatic flows. For this reason, the maps of two-phase flow structures for adiabatic flow, as well as for boiling and condensation, differ from each other. The limits of occurrence of individual structures are most often described using quantities such as void fraction ϕ , vapour quality x , mass flow density G , apparent velocity of individual phases j_v and j_l , as well as the Lockhart-Martinelli parameter χ_{tt} . These parameters allow for taking into account, in addition to the flow conditions, parameters characterizing heat transfer. The first structure map of two-phase nonadiabatic flow was published in 1980 by Breber et al. [16]. Maps for flow in conventional channels during condensation were also published by Soliman [17] and Teitela and Duklera [18]. These maps are most often modified by other authors.

In small diameter channels, viscosity forces and surface tension have a significant impact on the mechanism of momentum and energy change. The influence of gravity and inertia forces is less important here. These interactions cause the boundaries of the occurrence of individual flow structures to shift, which can be seen in Fig. 11 and Fig. 12.

Figure 11 shows the map published by El Hajal et al. [19] as well as its modifications for different heat flux densities compared with the Steiner map (Fig. 11b). Figure 12(a) shows the map by Coleman and Garimella [20], unlike the maps shown in Fig. 11 and Fig. 12b, this is a map for the condensation process. Figure 12b shows a comparison of flow structure maps by

Wojan et al. [21] and Yang et al. [22] for the boiling process of the R410A refrigerant in the channel $d = 6.3$ mm.

has been tested for the following refrigerants: R22, R134a, R290, R404a, R410a, R600, R507, R717, and R744 and compared with multi-author correlations. Figure 13 shows the Turgut and Akers map for the R22 and R10A refrigerants. One can see a change in the transition boundary between dry out and mist flow structures, as well as a shift in the boundary between intermittent flow and annular flow. The authors also observed similar shifts for other tested refrigerants.

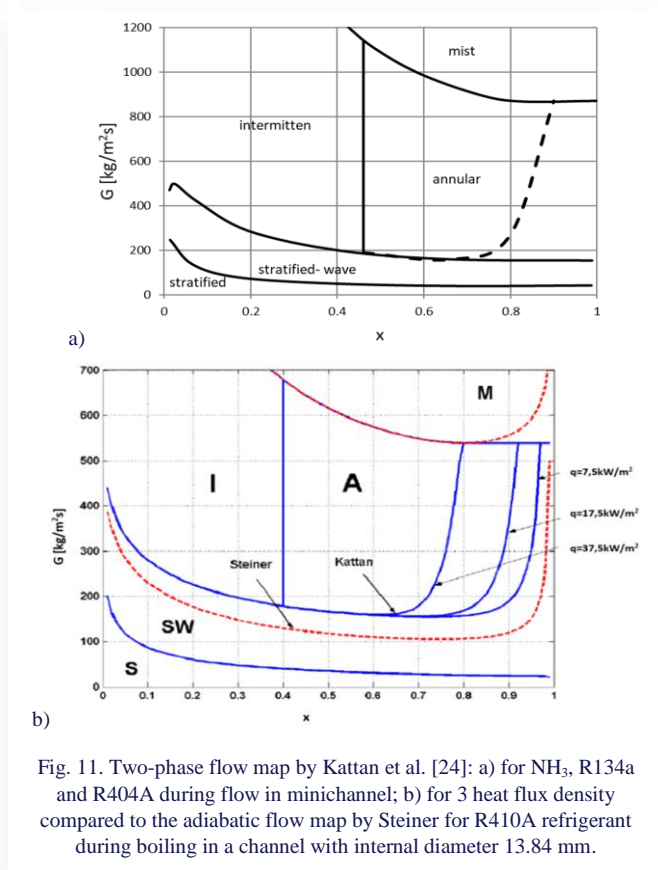


Fig. 11. Two-phase flow map by Kattan et al. [24]: a) for NH_3 , R134a and R404A during flow in minichannel; b) for 3 heat flux density compared to the adiabatic flow map by Steiner for R410A refrigerant during boiling in a channel with internal diameter 13.84 mm.

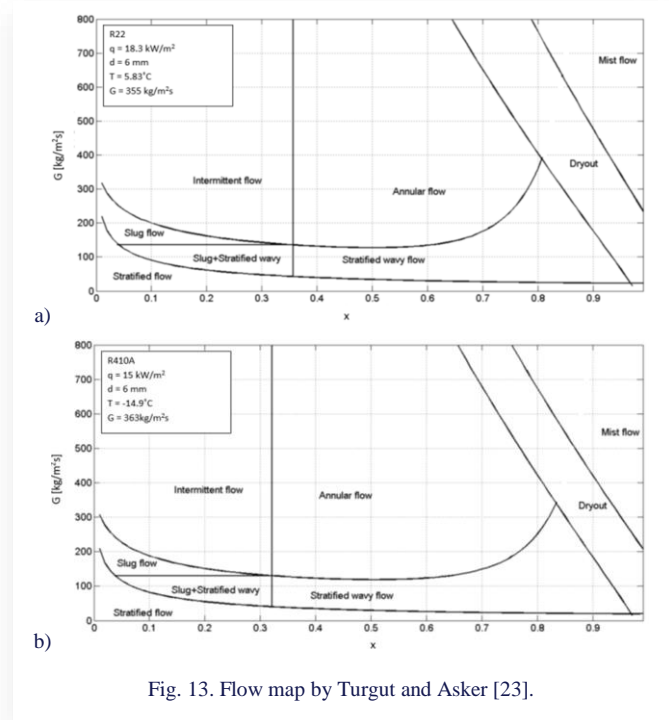


Fig. 13. Flow map by Turgut and Asker [23].

Unfortunately, the limits of the phase transition depend not only on the size of the channel or heat transfer but also on the refrigerant used, as presented by Nema et al. [25] (Fig. 14).

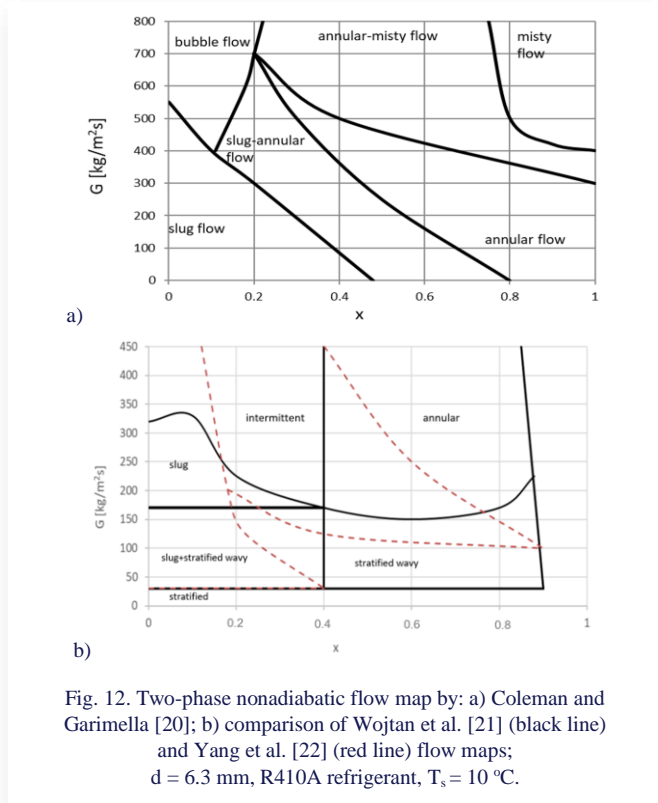


Fig. 12. Two-phase nonadiabatic flow map by: a) Coleman and Garimella [20]; b) comparison of Wojtan et al. [21] (black line) and Yang et al. [22] (red line) flow maps; $d = 6.3$ mm, R410A refrigerant, $T_s = 10$ °C.

Maps of flow structures for the boiling process were also published by Turgut and Asker [23]. This flow structure map

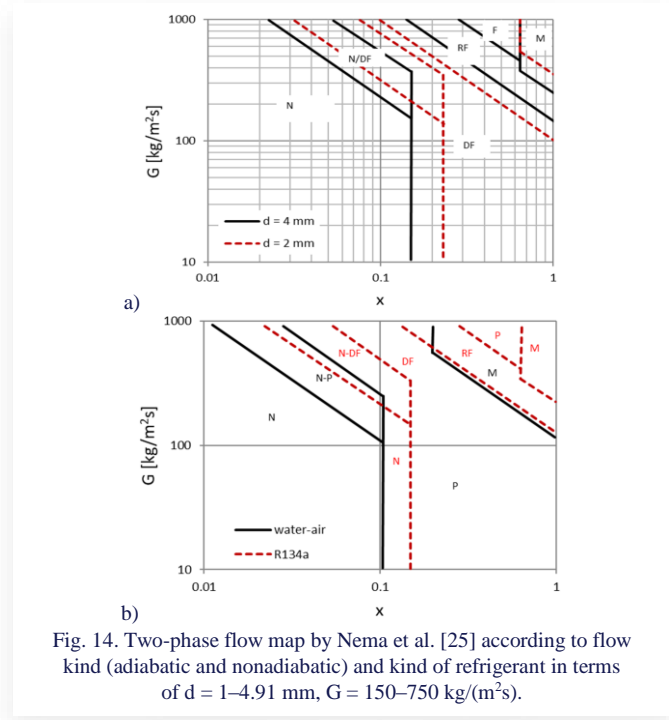


Fig. 14. Two-phase flow map by Nema et al. [25] according to flow kind (adiabatic and nonadiabatic) and kind of refrigerant in terms of $d = 1\text{--}4.91$ mm, $G = 150\text{--}750$ $\text{kg}/(\text{m}^2\text{s})$.

Figure 15a shows the map of Mishima et al. [26], which applies to two-phase flows in vertical gaps with a height in the range of 0.3–17 mm. The apparent velocities of the vapour and liquid phases were used to describe the transition boundaries of flow structures. This map applies to the following structures: bubbly, slug, frothy and annular, mist flow is not included here. This may be due to difficulties in observing this structure. Figure 15b shows the flow structure map of Sikora [27]. This is a map for two-phase condensation flow, constructed based on tests on the condensation of HFE7000, HFE7100 and Novec649 refrigerants in pipe minichannels with an internal diameter of less than 2 mm. To describe the limits, the author used the void fraction ϕ as a more universal value and less dependent on the properties of the refrigerant than the vapour quality. This is quite a detailed division compared to maps by other authors such as Wojtan or Yang (Fig. 12).

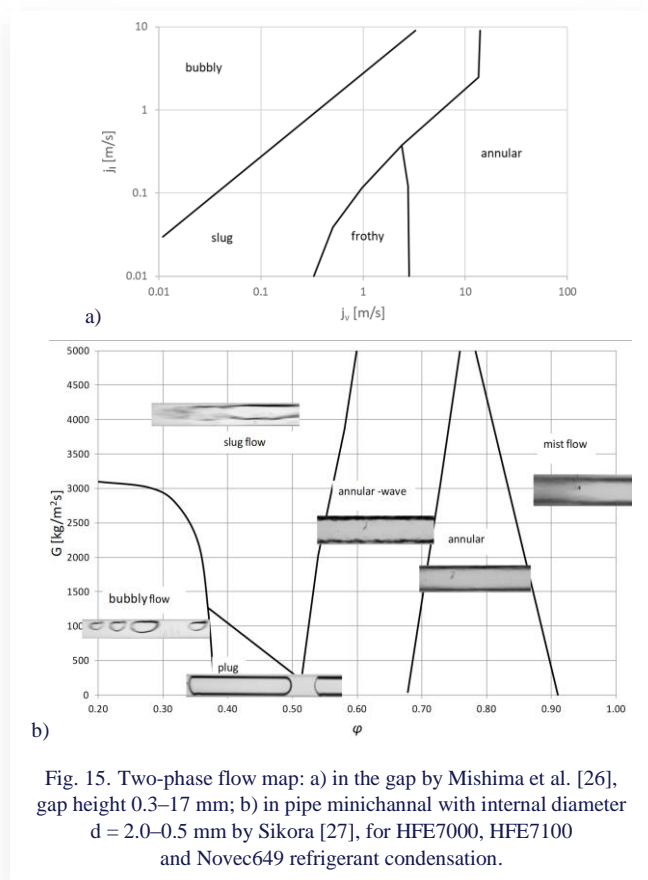


Fig. 15. Two-phase flow map: a) in the gap by Mishima et al. [26], gap height 0.3–17 mm; b) in pipe minichannel with internal diameter $d = 2.0\text{--}0.5$ mm by Sikora [27], for HFE7000, HFE7100 and Novec649 refrigerant condensation.

3. Three-phase Flow Structure Maps

There are two basic types of three-phase flow: two-component and three-component. In the case of a three-phase two-component mixture, two liquids and vapour one of them flow through the channel; in the case of a three-component flow, each phase is a different, mutually immiscible component. The three-phase flow of immiscible liquids and gas is characterized by high complexity, the interaction of phases at the interface and turbulence present in the flow make the process analysis difficult.

The first attempt to develop three-phase flow maps was made by Açıkgöz et al. [28]. They published three maps of three-phase flow in the system of apparent velocities of air and water.

Two of these maps are shown in Fig. 16. Since each of the maps published by Açıkgöz et al. is valid only for constant oil velocity, determining the type of structure for any flow conditions would be problematic and would require a very large number of maps.

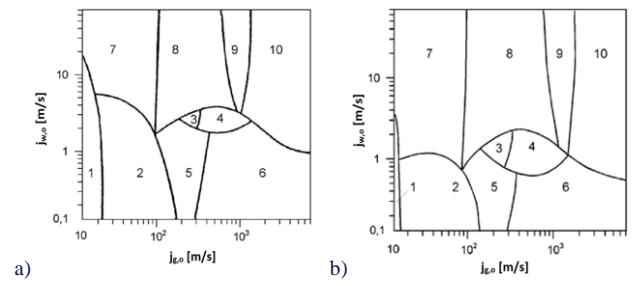


Fig. 16. Flow map of air-water-oil mixture: a) $j_{o,o} = 0.043$ m/s; b) $j_{o,o} = 0.09$ m/s according to Açıkgöz et al. [28] (Table 1 presents an explanation of the symbols)

Woods et al. [29] developed flow maps for the air-water-oil mixture for three apparent oil velocities ($j_{o,o} = 0.00475$ m/s, $j_{o,o} = 0.0794$ m/s, $j_{o,o} = 0.1673$ m/s), where the occurrence boundaries of the individual flow structures are marked. Examples of map constructions by Woods et al. are shown in Fig. 17.

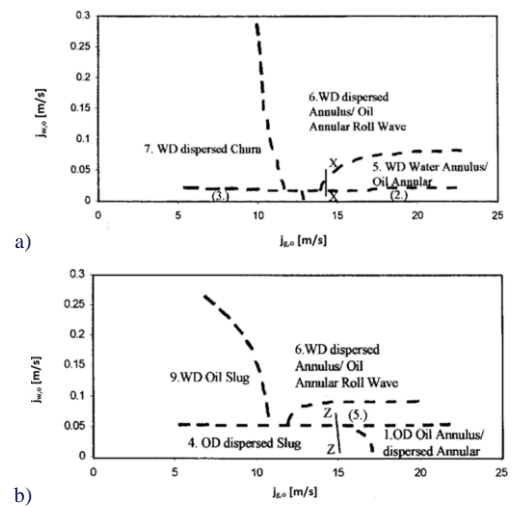


Fig. 17. Three-phase flow map of air-water-oil by Woods et al. [29] for oil velocity: a) $j_{o,o} = 0.00475$ m/s; b) $j_{o,o} = 0.1673$ m/s; (2.) – dispersed - annular flow, (3.) – dispersed - annular slight wave flow, (5.) – dispersive-semi-annular flow.

These maps were developed in a coordinate system including the apparent velocities of air and water, commonly used for two-phase flows, which means that the authors attempted to describe the three-phase flow as a classic two-phase gas-liquid flow. Woods et al. also proposed the following relationship:

$$j_{w,o} = 0.32j_{o,o} \quad (6)$$

to calculate the boundary between slug flows with the dominant oil and water phases.

Cazarez et al. [30] published a three-phase flow map based on their experimental research (Fig. 18a). It shows the areas

where pseudo-two-phase flow structures occur. In this case, the role of the liquid is played by a mixture of two heterogeneous liquids. The relationship between the velocities of individual components of a three-phase mixture and the apparent air velocity were used to describe the structures.

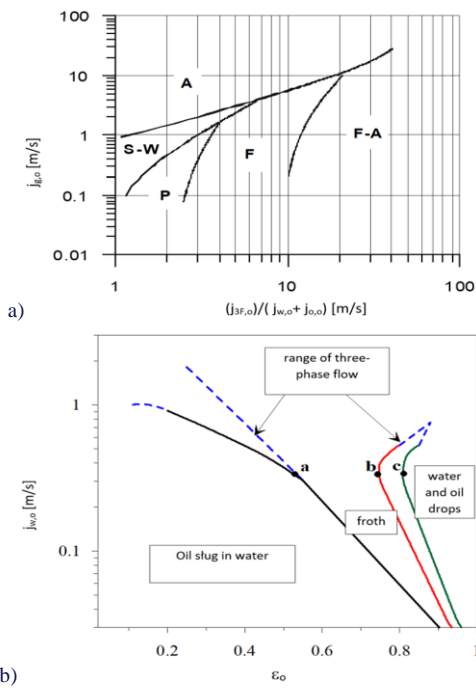


Fig. 18. Three-phase flow map by: a) Cazarez et al. [30]; b) Shean [31].
 A – annular flow; F – frothy flow; F-A – frothy - annular flow;
 P – plug flow; S-W – stratified – wave flow.

There are few published maps of three-phase ascending flow in the literature. One such map is Shean's map [31] (Fig. 18b). This map is an adaptation, for three-phase air-water-oil flow conditions, of the Govier end Aziz map [32] developed for vertical two-phase oil-water flow. The map was built in the coordinate system of the concentration of the oil phase in the liquid and the apparent velocity of water. The boundaries of the flow structures observed by the authors are marked with lines on the map. The authors justified the possibility of adapting Govier's map to the description of three-phase flow, taking into account the observed similarity in the course of the two- and three-phase total pressure loss curves, especially at critical points a, b, c (Fig. 18b). The modification consisted in expanding the area of slug and frothy flow with the dominant water phase. The limit value of oil concentration in the flow is determined using the relationship:

$$\varepsilon_{o,gr} = 0.6 + 0.315 \left\{ \tanh \left[0.272 \left(j_{g,o} - 17 \right) \right] + \tanh \left(17.25 - j_{g,o} \right) \right\} \quad (7)$$

However, Spedding et al. [33] presented three maps of three-phase flow (two of them are shown in Fig. 19), in which they marked the boundaries of the occurrence of three-phase structures. Table 1 presents an explanation of the symbols shown on Spedding's maps from Fig. 19. The apparent gas velocity and the concentration of oil in the liquid were used to describe the maps.

As can be seen in the maps, when the proportion of oil in water increases, the oil phase becomes dominant. Flow structures with a dominant water phase cover almost 40% of the map area. The increase in the velocity of the liquid above does not cause such visible changes in the phase dominance. The authors noticed that the location of the transition boundary between the dispersed-slug and dispersed-frothy structures does not change at a gas velocity of 2 m/s for all considered water velocities and low values of oil concentration in water.

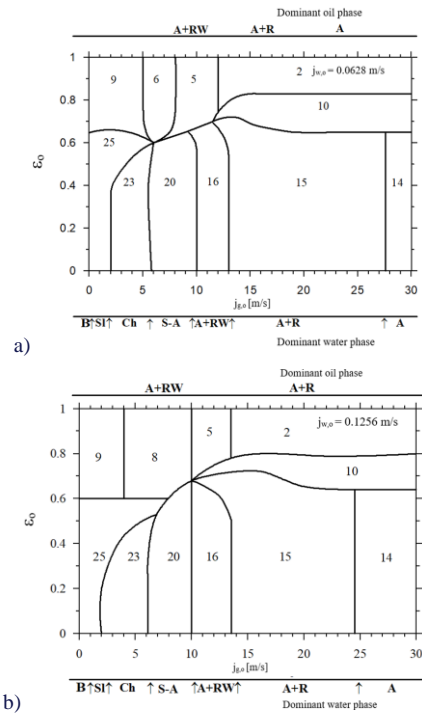


Fig. 19. Three-phase flow map for constant apparent velocity of water, by Spedding et al. [33]: a) $j_{w,o} = 0.0628$ m/s; b) $j_{w,o} = 0.1256$ m/s;
 B – bubbly, SI – slug, Ch – churn, S-A – semi-annular,
 A+RW – annular roll wave, A+R – annular ripple,
 dis A – dispersed annular, A – annular.

Table 1. Designations of three-phase flow structures for Figs. 16 and 19 [34].

| Dominant oil phase - OD | | Dominant water phase - WD | |
|-------------------------|---------------------------------------|---------------------------|--|
| 1 | oil-annular / dispersed-annular | 11 | water-annular oil-annular |
| 2 | dispersed-annular | 12 | water-annular/oil-annular slightly wavy |
| 3 | dispersed-annular, slightly wavy | 13 | water-annular/oil-annular strongly wavy |
| 4 | dispersed-annular, strongly wavy | 14 | dispersed-annular/oil-annular |
| 5 | dispersed-semi-annular | 15 | dispersed-annular/oil-annular slightly wavy |
| 6 | dispersed-semi-annular, strongly wavy | 16 | dispersed - annular/oil-annular, strongly wavy |
| 7 | dispersed-frothy | 17 | dispersed - annular |
| 8 | dispersed-annular/dispersed-plug | 18 | dispersed - annular, slightly wavy |
| 9 | dispersed-plug | 19 | dispersed - annular, strongly wavy |
| 10 | fracture-annular | 20 | dispersed - semi-annular |
| | | 21 | dispersed - semi-ring, slightly wavy |
| | | 22 | dispersed - semi-annular, strongly wavy |
| | | 23 | dispersed - frothy |
| | | 24 | dispersed - annular/dispersed-plug |
| | | 25 | dispersed - slug |
| | | 26 | oil-slug |

Figure 20 shows the investigation results of Pietrzak et al. [35] for three-phase flow, water – air - oil. As can be seen, structures for three-phase flow are more complicated than those for two-phase flow. There are more configurations of every fluid geometrical structure and it depends on the concentration of

every phase. The velocities of every phase influence the geometrical configuration of this phase. When the mass flow is very high, in this kind of multi-phase flow an emulsion can be formed. It is very hard to describe on one flow map.

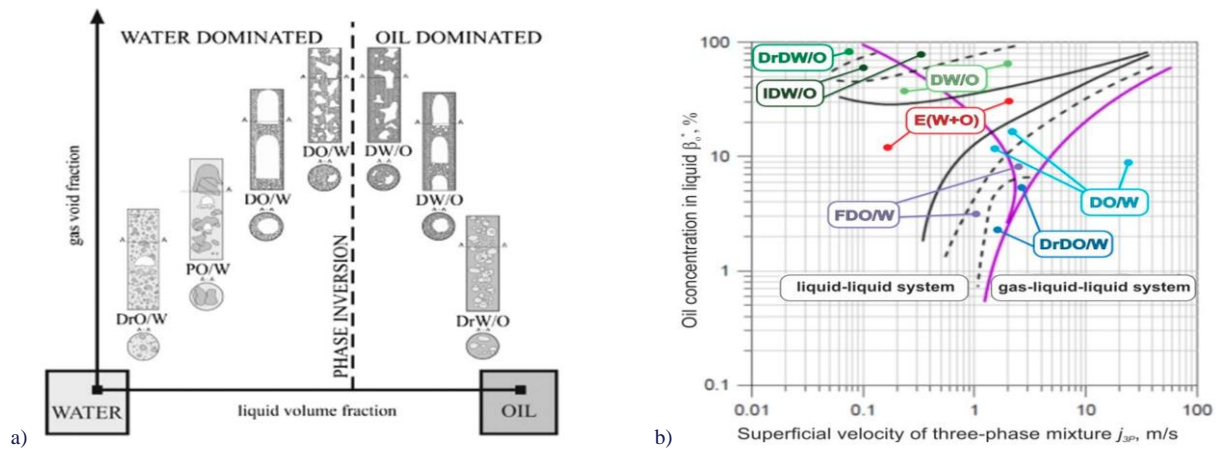


Fig. 20. Investigation results of Pietrzak et al. [35]: a) phase inversion in three-phase flow [35]; b) gas-liquid-liquid three-phase flow map for annular falling flow [36];

- B-DrO/W – gas bubbles (B) and drops of oil (DrO) in water continuum (W).
- B-PO/W – gas bubbles (B) and plugs of oil (PO) in water continuum (W).
- P-DrO/W – plugs of gas (P) and discrete oil droplets (DrO) in water continuum (W).
- F-DO/W – breaking up and coalescence of gas bubbles; irregularly shaped gas bubbles flowing with high velocity; an oscillating fluid flow contributes to the formation of multi-phase mixture with froth characteristics (F); oil is dispersed (DO) in water continuum (W).
- A-DO/W – annular (A) air-liquid mixture flow; oil dispersed (DO) in water (W).
- B-DrW/O – gas bubbles (B) and drops of water (DrW) in oil continuum (O).
- P-DrW/O – gas plugs (P) and drops of water (DrW) in oil continuum (O).
- F-DW/O – breaking and connecting gas bubbles with irregularly shape flowing at a high velocity, with an oscillating fluid flow contributes to the formation of multi-phase mixture with foam characteristics (F); water dispersed (DW) in oil continuum (O).
- A-DW/O – annular (A) air-liquid mixture flow; water dispersed (DW) in oil (O).

4. Summary and conclusions

To sum up, the occurrence of multiphase flow structures depends on several phases and affects the functioning of many flow machines. Therefore, flow structure maps are a very important tool for both scientists and engineers, they allow determining flow conditions only by measuring a few basic parameters such as flow rate, pressure, temperature and flow speed. Unfortunately, there are no unified maps, so we have to look for maps prepared for the fluid used in a given process. Based on the analysed literature, several conclusions can be drawn:

1. Maps of multiphase flow structures are the best tool to determine the flow structures occurring in given conditions. They are simple and allow to select the appropriate model to determine the heat transfer coefficient and the flow resistance of the fluid. This has a major impact on the design of refrigeration and air conditioning equipment.
2. For flow structure maps to be useful in practice, they should be as generalized as possible, and the boundaries of individual structures' occurrence should be described using parameters that are easy to determine in practice. As can be seen, the use of complex quantities makes the practical use of maps of multiphase flow structures difficult. To construct a good flow map it is necessary to connect a lot of flow and heat parameters, which is difficult.

3. The type of multiphase flow structure depends primarily on the diameter of the channel, the orientation of its axis, the type of fluid, its concentration and density, and process parameters (saturation pressure and temperature, mass flow density, phase velocity, heat flux density). These quantities influence the balance of forces acting on all phases and their interface surfaces, as well as the vapour quality x , the void fraction of the channel ϕ , and define the share of the number of phases flowing through the channel.
4. Unfortunately, there are many discrepancies in the literature as to the scope of occurrence of individual flow structures in given conditions, therefore efforts should be made to simplify and standardize the construction of maps of multiphase flow structures.

References

- [1] Sikora, M. (2020). *Modeling of two-phase flow structures during condensation in mini-channels*. Koszalin University of Technology (in Polish).
- [2] Dziubiński, M., & Prywer, J. (2009). *Two-phase fluid mechanics*. Scientific and Technical Publishing House, Warsaw (in Polish).
- [3] Ulbrich, R. (2014). *Modern research methods for flows in multiphase systems*. Publishing House of the Opole University of Technology (in Polish).

- [4] Zhang, J., Xu, J.Y., Wu, Y.X., Li, D.H., & Li, H. (2013). Experimental validation of the calculation of phase holdup for an oil–water two-phase vertical flow based on the measurement of pressure drops. *Flow Measurement and Instrumentation*, 31, 96–101. doi: 10.1016/j.flowmeasinst.2012.08.002
- [5] Bannwart, A.C., Rodriguez, O.M.H., Trevisan, F.E., Vieira, F.F., & de Carvalho, C.H.M. (2009). Experimental investigation on liquid–liquid–gas flow: Flow patterns and pressure-gradient. *Journal of Petroleum Science and Engineering*, 65(1–2), 1–13. doi: 10.1016/j.petrol.2008.12.014
- [6] Plączek, M., Pietrzak, M., & Witeczak, S. (2018). A conductometric method for determining the upward gas-liquid-liquid three-phase flow. *Archives of Thermodynamics*, 39(3), 97–110. doi: 10.1515/aoter-2018-0022
- [7] Baker, O. (1954). Simultaneous flow of oil and gas. *Oil and Gas Journal*, 53, 185–190.
- [8] Charles, M.E., Govier, G.W., & Hodgson, G.W. (1961). The horizontal pipeline flow of equal density oil-water mixtures. *Canadian Journal of Chemical Engineering*, 39, 27–36. doi: 10.1002/cjce.5450390106
- [9] Troniewski, L., Witeczak, S., & Trębacz, J. (2000). Two-phase water-oil flow in vertical channels. *Science Notebooks Mechanics. Opole University of Technology*, 65, 39–54 (in Polish).
- [10] Xu, J., Li, D., Guo, J., & Wu, Y. (2010). Investigations of phase inversion and frictional pressure gradients in upward and downward oil–water flow in vertical pipes. *International Journal of Multiphase Flow*, 36, 930–939. doi: 10.1016/j.ijmultiphaseflow.2010.08.007
- [11] Flores, J.G. (1997). *Oil–Water Flow in Vertical and Deviated Wells*. University of Tulsa.
- [12] Brandt, A. (2014). *Annular flow of a multiphase mixture in the pipes of thin-film apparatus*. PhD thesis, Opole University of Technology (in Polish).
- [13] Hewitt, G.F., & Roberts, D.N. (1969). *Studies of Two-Phase Flow Patterns by Simultaneous X-Ray and Flash Photography*. Berkshire: Atomic Energy Research Establishment. Harwell, England.
- [14] Taitel, Y., & Dukler, A.E. (1976). A model for predicting flow regime transitions in horizontal and near horizontal gas-liquid flow. *AIChE Journal, American Institute of Chemical Engineers*, 22(1), 47–55. doi: 10.1002/aic.690220105
- [15] Ulbrich, R. (1989). *Identification of two-phase gas-liquid flow*. Studies and Monographs, 32, WSI, Opole (in Polish).
- [16] Breber, G., Palen, J.W., & Taborek, J. (1980). Prediction of Horizontal Tubeside Condensation of Pure Components Using Flow Regime Criteria. *Journal of Heat Transfer*, 102, 471–476. doi: 10.1115/1.3244325
- [17] Soliman, H.M. (1982). On the annular-to-wavy flow pattern transition during condensation inside horizontal tubes. *Canadian Journal of Chemical Engineering*, 60, 475–481. doi: 10.1002/cjce.5450600405
- [18] Taitel, Y., & Dukler, A.E. (1976). A model for predicting flow regime transitions in horizontal and near horizontal gas-liquid flow. *AIChE Journal, American Institute of Chemical Engineers*, 22, 47–55. doi: 10.1002/aic.690220105
- [19] El Hajal, J., Thome, J.R., & Cavallini, A. (2003). Condensation in horizontal tubes, part 1: two-phase flow pattern map. *International Journal of Heat and Mass Transfer*, 46, 3349–3363. doi: 10.1016/S0017-9310(03)00139-X
- [20] Coleman, J.W., & Garimella, S. (2003). Two-phase flow regimes in round, square and rectangular tubes during condensation of refrigerant R134a. *International Journal of Refrigeration*, 26, 117–128. doi: 10.1016/S0140-7007(02)00013-0
- [21] Wojtan, L., Ursenbacher, T., & Thome, J.R. (2005). Investigation of flow boiling in horizontal tubes: Part I—A new diabatic two-phase flow pattern map. *International Journal of Heat and Mass Transfer*, 48, 2955–2969. doi: 10.1016/j.ijheatmasstransfer.2004.12.012
- [22] Yang, C.M., & Hrnjak, P. (2020). A new flow pattern map for flow boiling of R410A in horizontal micro-fin tubes considering the effect of the helix angle. *International Journal of Refrigeration*, 109, 154–160. doi: 10.1016/j.ijrefrig.2019.09.013
- [23] Turgut, O.E., & Asker, M. (2022). Flow boiling behaviors of various refrigerants inside horizontal tubes: a comparative research study. *Eskişehir Technical University Journal of Science and Technology A - Applied Sciences and Engineering*, 23, 1–20. doi: 10.18038/estubtda.749040
- [24] Kattan, N., Thome, J.R., & Favrat, D. (1998). Flow Boiling in Horizontal Tubes: Part 1—Development of a Diabatic Two-Phase Flow Pattern Map. *Journal of Heat Transfer*, 120, 140. doi: 10.1115/1.2830037
- [25] Nema, G., Garimella, S., & Fronk, B.M. (2014). Flow regime transitions during condensation in microchannels. *International Journal of Refrigeration*, 40, 227–240. doi: 10.1016/j.ijrefrig.2013.11.018
- [26] Mishima, K., Hibiki, T., & Nishihara, H. (1993). Some characteristics of gas-liquid flow in narrow rectangular ducts. *International Journal of Multiphase Flow*, 19, 115–124. doi: 10.1016/0301-9322(93)90027-R
- [27] Sikora, M. (2021). Flow Structure Investigations during Novec Refrigerant Condensation in Minichannels. *Materials*, 14, 6889. doi: 10.3390/ma14226889
- [28] Açıkgöz, M., França, F., & Lahey, R.T. (1992). An experimental study of three-phase flow regimes. *International Journal of Multiphase Flow*, 18, 327–336. doi: 10.1016/0301-9322(92)90020-H
- [29] Woods, G.S., Spedding, P.L., Watterson, J.K., & Raghunathan, R.S. (1998). Three-Phase Oil/Water/Air Vertical Flow. *Chemical Engineering Research and Design*, 76, 571–584. doi: 10.1205/026387698525252
- [30] Cazarez, O., Montoya, D., Vital, A.G., & Bannwart, A.C. (2010). Modeling of three-phase heavy oil–water–gas bubbly flow in upward vertical pipes. *International Journal of Multiphase Flow*, 36, 439–448. doi: 10.1016/j.ijmultiphaseflow.2010.01.006
- [31] Shean, A.R. (1976). *Pressure drop and phase fraction in oil-water-air vertical pipe flow*. Thesis, Department of Mechanical Engineering, Massachusetts Institute of Technology, Cambridge.
- [32] Govier, G.W., & Aziz, K. (2008). *The Flow of Complex Mixtures in Pipes*. (2nd Edn.). Society of Petroleum Engineers.
- [33] Spedding, P.L., Woods, G.S., Raghunathan, R.S., & Watterson, J.K. (2000). Flow Pattern, Holdup and Pressure Drop in Vertical and Near Vertical Two- and Three-Phase Upflow. *Chemical Engineering Research and Design*, 78, 404–418. doi: 10.1205/026387600527301

- [34] Nowak, M. (2007). *Volume share and resistance of three-phase flow in the vertical channel*. Opole University of Technology (in Polish).
- [35] Pietrzak, M., Płaczek, M., & Witzak, S. (2017). Upward flow of air-oil-water mixture in vertical pipe. *Experimental Thermal and Fluid Science*, 81, 175–186. doi: 10.1016/j.expthermflusci.2016.10.021
- [36] Brandt, A., Czernek, K., Płaczek, M., & Witzak, S. (2021). Downward Annular Flow of Air–Oil–Water Mixture in a Vertical Pipe. *Energies*, 14(1), 30. doi: 10.3390/en14010030